

# TWO-PARTICLE RESONANT STATES IN A MANY-BODY MEAN FIELD

R. Id Betan <sup>a,b)</sup>, R. J. Liotta <sup>a)</sup>, N. Sandulescu <sup>a,c)</sup>, T. Vertse <sup>a,d)</sup>

<sup>a)</sup> Royal Institute of Technology, SCFAB, SE-10691, Stockholm, Sweden

<sup>b)</sup> Departamento de Fisica, FCEIA, UNR, Avenida Pellegrini 250,  
2000 Rosario, Argentina

<sup>c)</sup> Institute of Physics and Nuclear Engineering,  
P.O.Box MG-6, Bucharest-Magurele, Romania

<sup>d)</sup> Institute of Nuclear Research of the Hungarian Academy of Sciences,  
H-4001 Debrecen, Pf. 51, Hungary

## Abstract

A formalism to evaluate the resonant states produced by two particles moving outside a closed shell core is presented. The two particle states are calculated by using a single particle representation consisting of bound states, Gamow resonances and scattering states in the complex energy plane (Berggren representation). Two representative cases are analysed corresponding to whether the Fermi level is below or above the continuum threshold. It is found that long lived two-body states (including bound states) are mostly determined by either bound single-particle states or by narrow Gamow resonances. However, they can be significantly affected by the continuum part of the spectrum.

PACS number(s): 25.70.Ef,23.50.+z,25.60+v,21.60.Cs

The prospect of reaching and measuring very unstable nuclei, as is materializing now, opens the possibility of studying spectroscopic processes occurring in the continuum part of nuclear spectra. Much work has already been done in this subject, particularly regarding halo nuclei [1]. Still, the role played by single-particle resonances and of the continuum itself upon particles moving in the continuum of a heavy nucleus is not fully understood. For instance, one may wonder whether two particles outside a core where the Fermi level is immersed in the continuum may produce a quasibound state and, in this case, whether that state is built upon narrow single-particle resonances or by an interplay between the two-particle interaction and the continuum, or by a combination of these mechanisms, as it happens in typical halo nuclei. To answer such questions is a difficult undertaking, particularly because the resonances on the real energy axis do not correspond to a definite state. A way of approaching this problem is by solving the Schrödinger equation with outgoing boundary conditions. One thus obtains the resonances as poles of the S-matrix in the complex energy plane. These poles (Gamow resonances) can be considered discrete states on the same footing as bound states (see Ref. [2] and references therein). However, in this case one finds that physical quantities, like energies and probabilities, become complex. One may attempt to give meaning to these complex quantities. Thus, it is usually assumed that the imaginary part of the energy of a decaying resonance is (except a minus sign) half the width. Other examples are the interpretation of complex cross sections done by Berggren [3] or the widely used radioactive decay width evaluated by Thomas as the residues of the S-matrix [4]. All these interpretations are valid only if the resonances are isolated and, therefore, narrow. In this case the residues of the S-matrix becomes real. One may thus apply this theory and evaluate all resonances, giving physical meaning to the narrow ones only. To achieve this goal a representation consisting of bound states, Gamow resonances and the proper continuum was proposed some years ago [2] (Berggren representation). One chooses the proper continuum as a given contour in the complex energy plane and forms the basis set of states (the representation) as the bound states plus the Gamow resonances included in that contour plus the scattering states on the contour [2].

Using the Berggren representation one can evaluate any one-particle quantity in the complex energy-plane, e. g. the eigenstates of a deformed potential in terms of the Berggren states provided by a spherical basis. One may thus think that the Berggren representation can also be used straightaway to evaluate many-particle quantities, as one does with the shell-model using bound representations. Unfortunately this is not the case. The root of the problem is that the set of energies of the two-particle basis states may cover the whole complex energy plane of interest. To show this we will analyse the relatively simple case of two particles outside a core in terms of the Green function. For clarity of presentation we will give here the main points of the derivations leading to the Berggren representation.

The single-particle Green function in the complex energy plane can be written as [5]

$$g(r, r'; E) = \sum_{n=1}^{N_d} \frac{w_n(r)w_n(r')}{E - \epsilon_n} + \int_{L^+} d\epsilon \frac{u(r, \epsilon)u(r', \epsilon)}{E - \epsilon} \quad (1)$$

where  $L^+$  is an integration path on the complex energy plane and  $u(r, \epsilon)$  is the corresponding scattering function. The index  $n$  labels the bound states and Gamow resonances which lie between the real energy axis and the integration path and  $w_n(r)$  are the corresponding wave functions, i. e. the outgoing solutions of the Schrödinger equation. The total number

of bound plus Gamow states, i. e. of discrete states, is  $N_d$ . Notice that the Berggren metric in Eq. (1) corresponds to the product of a function times itself, and not times its complex conjugate. This induces the complex probabilities mentioned above. But on the real energy axis (where the scattering functions can be chosen to be real) the Berggren and Hilbert internal products coincide. Therefore, since this formalism is based upon a Cauchy transformation to the complex energy plane, it should provide at the same time the physical complex quantities mentioned above plus the real ones as evaluated by using bound representations, e. g. within the shell model. This is a strong constraint that will help us to probe the formalism and check the computer codes.

The numerical evaluation of the integral requires the discretization of the complex energy  $\epsilon$  along the integration contour. We will use the Gauss integration method with a total number of integration points  $N_g$  and weights  $h_p$ . This defines the Berggren representation, i. e. the set of orthonormal (in the Berggren metric) basis vectors  $\{|\varphi_j\rangle\}$  given by the set of bound and Gamow states  $\{\varphi_p(r)\} = \{w_p(r)\}$  and the discretized scattering states  $\{\varphi_p(r)\} = \{\sqrt{h_p}u(r, \epsilon_p)\}$ . The single particle Green function can then be written as

$$g(r, r'; E) = \sum_{p=1}^N \frac{\varphi_p(r)\varphi_p(r')}{E - \epsilon_p} \quad (2)$$

where  $N = N_d + N_g$ .

The two-particle Green function is [6],

$$G(r, r'; E) = G_0(r, r'; E) + \int dr_1 dr_2 G_0(r, r_1; E) V(r_1 r_2) G(r_2, r'; E) \quad (3)$$

where  $G_0$  is the bare (zeroth-order) two-particle Green function which within the Berggren representation reads,

$$G_0(r, r'; E) = \sum_{i \leq j=1}^N \frac{\varphi_i(r)\varphi_j(r)\varphi_i(r')\varphi_j(r')}{E - (\epsilon_i + \epsilon_j)} \quad (4)$$

As seen from Eq. (3), in order to obtain the poles and residua (i. e. energies and wave functions) of the correlated two-particle Green function one has to assume that they do not coincide with those in the zeroth-order Green function [6]. But by choosing an arbitrary path for the one-particle scattering states in the complex energy plane, one may obtain a continuum plane of zeroth-order poles corresponding to the sum  $\epsilon_i + \epsilon_j$ . Therefore, in this plane one would not be able to evaluate any two-particle pole.

As an illuminating example we show in Fig. 1(a) a rectangular one-particle contour without any discrete state. From Eq. (4) one sees that in the complex two-particle energy plane the zeroth-order energies are given by the geometrical sum of a point  $i$  on the one-particle contour (corresponding to the complex energy  $\epsilon_i$ ) plus another point  $j$  on that contour, such that  $i \leq j$ . These energies are located in the two-particle complex energy plane as shown in Fig. 1(b). For example, the dashed region located between  $a$  and  $2a$  on the real energy axis is produced by one of the particles lying in the first segment of the one-particle contour, i. e. with energy  $\epsilon_i = (x, 0)$  such that  $0 < x < a$ , and the second particle in the segment with energy  $\epsilon_j = (a, y)$  such that  $-c < y < 0$ . Therefore the zeroth-order two-particle energy is  $\epsilon_i + \epsilon_j = (x + a, y)$ , which covers the region mentioned above. The

rest of the dashed plane in Fig. 1(b) is produced in the same fashion, with the energies of the particles on different segments of the one-particle contour.

We thus see that if  $2a < b$  then there is a region in the two-particle complex energy plane which is free from any uncorrelated solution. Therefore, in this region one can search for resonant states of the interacting two-particle system. By choosing the real energies  $a$  and  $b$  conveniently, i. e. such that  $2a < b$  as in Fig. 1(b), one can study two-particle resonances lying in any reasonable energy region. We will call this the "allowed" energy region.

The allowed region in the two-particle complex energy plane plays a role similar to the contour in the one-particle energy plane. That is, only those one-particle resonances with complex energies that lie between the real energy axis and the contour can be evaluated by using the Berggren representation [2]. In the same fashion, only those two-particle resonant states with complex energies contained in the allowed region can be evaluated within that representation.

The allowed region can be determined by fulfilling some physically meaningful requirements. Thus, one expects that the single-particle resonances and the continuum scattering states closest to threshold would play an important role in the building up of correlated low lying two-particle states. Therefore they should be included in the basis, which implies that the one-particle contour of Fig. 1(a) should correspond to small values of  $a$  and large values of  $b$ , as indeed is the case in Fig. 1(b).

Using the Berggren representation one can obtain the two-particle TDA equations in a standard fashion. We will use in our derivations separable forces so that those equations convert into the usual dispersion relation [7,8], i. e.

$$-1/G_\lambda = \sum_{i \leq j} \frac{C^2(ij, \lambda)}{E - \epsilon_i - \epsilon_j} \quad (5)$$

where  $E$  is the complex energy of the two-particle states carrying angular momenta  $\lambda$ ,  $C(ij, \lambda)$  is the  $\lambda$ -multipole component of the interaction while  $i$  and  $j$  label the single-particle states with complex energies  $\epsilon$  corresponding to our Berggren representation. For a detailed expression of the coefficient  $C(ij, \lambda)$  see, e. g., Eq. (32) of Ref. [8]. It contains the matrix element of the radial field  $f_\lambda(r)$  in the separable interaction, i. e.  $\int r^2 dr \varphi_i(r) f_\lambda(r) \varphi_j(r)$ . Notice again the Berggren metric in the radial internal products and that it is the square (and not the absolute value square) of the matrix elements that appear in the dispersion relation.

To generate the single-particle states we will use a Woods-Saxon potential (WS). The field  $f_\lambda$  is the derivative of the WS. It may be argued that this interaction is too simple to describe the motion of the particles in the continuum and that a more realistic force should be used, as it was done, e. g., in Ref. [9]. However, our purpose here is not to explain in detail processes happening in the continuum, but rather to understand the role played by the various ingredients entering into the two-particle quasibound state that may be built as a result of the interplay among those ingredients. We assume that this process occurs near the nuclear surface and, therefore, our separable force should be suitable for the analysis that we intend to carry out.

We will apply the formalism presented here to analyse neutron excitations in a nucleus that would lie on or even beyond the drip line. That is, the Fermi level may be close to or even immersed in the continuum. We will analyse these two possibilities separately.

The calculation of the bound states and the Gamow resonances will be performed by using an updated version of the compute code GAMOW [10] while the scattering waves on the complex contour of Fig. 1(a) will be evaluated by using the computer code ZSCAT [11].

The WS to be used correspond to the double closed shell nucleus  $^{78}\text{Ni}$ . The parameters for the volume part of the interaction are  $V_0 = 40\text{MeV}$ ,  $r_0 = 1.27\text{fm}$ ,  $a = 0.67\text{fm}$ . The spin-orbit interaction has the same values of  $r_0$  and  $a$ , but the depth of the potential is  $V_{so} = 21.43\text{MeV}$ . With these parameters one obtains the single-particle states shown in Table I under the label *WS1*. They are quite similar to the ones given by a Skyrme-HF calculations [12]. The shell  $N = 50$  is well defined, since there is a gap of about 3.6 MeV between the lowest particle state, which here is  $1d_{5/2}$ , and the highest hole state, i. e.  $0g_{9/2}$ .

We will also evaluate a case where no bound single-particle states are present. For this, we reduced the value of the depth of the WS to  $V_0 = 37\text{MeV}$ . The corresponding single-particle states are shown under the column *WS2* in Table I. One sees that with this rather shallow potential the gap corresponding to  $N = 50$  is still present, given credibility to our TDA calculation. It is also to be noticed that the particle state  $2s_{1/2}$  has disappeared, as expected for neutron excitations.

We will here present two-particle states with angular momentum  $\lambda = 0$ , for which the separable force is known to reproduce well experimental data when available. We will first analyse the case where there are bound single-particle states, i. e. the case *SW1* in Table I. To determine the strength of the separable force we will follow the standard procedure of adjusting  $G_\lambda$  by fitting the energy of a two-particle state, which usually is experimentally known. In our case we will assume that such state, which would be the ground state of  $^{80}\text{Ni}$ , exists below twice the energy of the lowest single particle state, i. e. below  $2\epsilon_{1d_{5/2}}$ . This energy gap, i. e. the correlation energy, is more than 1 MeV in well established normal nuclei, like  $^{208}\text{Pb}$  (where it is 1.244 MeV) and  $^{56}\text{Ni}$  (1.936 MeV). However in our case the bound states are so few and so slightly bound that such high energy gaps do not seem to be reasonable. Since there is not any experimental data which could guide us, and since our intention is just to see how the strength of the force affects the results, we will vary the gap from a value of only 300 keV to the rather large value of 1.7 MeV to examine the differences.

The values of  $G_\lambda$  thus obtained depends upon the number of states included in the basis, as can be seen from Eq. (5). In the calculations to be presented here we used a rectangular contour with the vertices as in Fig. 1(a) with  $a=0.5$  MeV,  $b=9$  MeV,  $c=-4$  MeV and  $d=20$  MeV. We thus include in the Berggren basis all the bound and Gamow states shown in Table I (except, of course, the hole state  $0g_{9/2}$ ). The allowed region, therefore, comprises the two-particle energy plane with complex energies  $(E_r, E_i)$  such that  $1\text{MeV} < E_r < 9\text{MeV}$  and  $-4\text{MeV} < E_i < 0\text{MeV}$ .

As in Ref. [2] we use a Gaussian method of integration over the contour. The corresponding Gaussian points provide the scattering waves constituting the basis elements on the continuum. We have found that in order to obtain convergence within six digits in the evaluated quantities, one has to include 10 Gaussian points for each MeV on the lines of the contour, except for the last segment (the one going from  $(b,0)$  to  $(d,0)$ ) where 5 points for each MeV is enough. We arrive to this conclusion by always choosing the contour such that the resonances lie at least 300 keV from the borders of the contour. The number of scattering states thus included in the basis is  $N_g=225$ . In Table II we show the convergence of the results as a function of  $N_g$  as well as the influence of the continuum upon the calculated

states. We will come back to this point below.

One can check the reliability of the results by performing a calculation over the real energy axis only [9]. The real (bound) energies thus obtained, which we call "exact", should coincide with those evaluated by using any contour. Moreover, the value of  $G_\lambda$  should, in all cases, be a real quantity. All these requirements are indeed fulfilled in our calculations.

In Fig. 2 we present all the calculated energies which we found inside the allowed region of the complex two-particle plane. The strength of the separable force was evaluated assuming that the energy gap is 1.4 MeV, i. e. the ground state energy is -3 MeV.

The first feature that strikes the eye in this figure is the straight line pattern that follow most of the energy points. These lines correspond to basis states where one of the particles moves in a bound or Gamow state and the other in a fragment of the one-particle contour. For instance, the straight line at a real energy of 3.796 MeV corresponds to a particle in the Gamow state  $0h_{11/2}$ , with an energy (3.296,-0.013) MeV (as seen in Table I), while the other is in the  $h_{11/2}$  scattering states lying on the border at  $a=0.5$  MeV in the contour of Fig. 1(a). The sum of both single-particle energies yields a real part of 3.796 MeV, which shows that these states are in fact poles of the zeroth-order Green function. Similar structures are found for all the straight lines in this figure, with the single-particle quantum numbers as indicated in the end of the lines. Thus, the horizontal segment at -0.479 MeV corresponding to the configuration  $d_{3/2}^2$  is produced by a particle in the Gamow state  $1d_{3/2}$  while the other is on the scattering states belonging to the segment of the contour on the real energy axis between 0 and  $a=0.5$  MeV. This horizontal segment does not appear in the lines labelled  $d_{5/2}^2$  and  $s_{3/2}^2$  in Fig. 2 because this lines are generated by the bound single-particle states coupled to the scattering states on the border of the contour lying between (b,0) and (b,-c) in Fig. 1(a).

We found that all the lines in Fig. 2 correspond to zeroth-order poles. Therefore the states on the lines are solutions of both the correlated and the uncorrelated two-particle Hamiltonian. They do not describe the physical resonances that we are searching and can be considered spurious states. This peculiar feature of the continuum is also found in the one-particle case, where the states lying on the contour are solutions of both the correlated and the uncorrelated one-particle Hamiltonian, as it was shown in Ref. [2].

Besides these peculiar lines the only two-particle states inside the allowed region are those indicated by open circles. These states include the two bound states at -3 MeV and -0.653 MeV as well as a number of resonances. They are mainly generated by configurations where both particles occupies bound states and/or Gamow resonances. To show the effect of the interaction upon these states, which are the physical ones, we present in Fig. 3 the corresponding energies as a function of the energy gap that defines  $G_\lambda$ . The surprising feature in this figure is that all the states become narrower as the interaction increases, except the state that in zeroth-order is the narrowest one, i. e.  $h_{11/2}^2$ .

The wave function amplitude corresponding to a given configuration is in our case proportional to the degeneracy of the configuration. Therefore the configuration  $h_{11/2}^2$  should be decisive in the building up of narrow two-particle resonances, both because it is the one with largest degeneracy and also because in zeroth-order it is the narrowest state. Another feature of our separable force is that that wave function amplitude becomes more important as the correlated energy approaches the configuration (zeroth-order) energy. This indeed happens in our case, as can be seen in Table III, where the value of the wave function am-

plitude  $X((0h_{11/2})^2; E)$  is given for the resonances in Fig. 3. One sees that as the states become narrower the shell  $0h_{11/2}$  becomes more important in the corresponding wave functions. And the other way around: the states labelled  $h_{11/2}^2$  becomes wider as the interaction increases while the shell  $0h_{11/2}$  becomes less important.

An important conclusion that can be drawn from Fig. 3 is that due to the two-particle interaction wide resonances can give rise to narrow ones. This is shown by the states  $g_{7/2}^2$  and  $d_{3/2}^2$ , although here one sees that the width of the resonance diminishes to reach a minimum value at  $\Delta = 1.4$  MeV and after that it starts to increase again. Even the states  $g_{7/2}^2$  and  $f_{7/2}^2$  reach a point where increasing  $\Delta$  does not affect the energies much. A result of this is that the corresponding wave function components  $X((0h_{11/2})^2; E)$  also remain unchanged, as seen in Table III. The bound states behave in a standard shell model fashion, as expected for bound states. In particular the states labelled  $s_{1/2}^2$ , where the low degeneracy shell  $2s_{1/2}$  is dominant, are weakly affected by the interaction.

Although the physical states presented above are mainly determined by discrete states, the continuum part of the spectrum plays also an important role. In particular, one can see in Table II that the energies evaluated by excluding the scattering states do not fit well the correct results. It is also important to mention that in our calculations we require the Hamiltonian to be Hermitian, which implies that the strength  $G_\lambda$  has to be a real quantity.<sup>1</sup> But by fitting the energy of  $^{80}\text{Ni}(\text{gs})$  to the value -3 MeV (i. e.  $\Delta = 1.4$  MeV) and excluding the continuum,  $G_\lambda$  becomes complex. By taking the corresponding real part only, as was done in Table II, that ground state energy acquires the unphysical value (-2.856,0.359) MeV. Even the energy of the (bound) first excited state  $E_1$  is unphysical since its energy is not real and the first resonance, i. e.  $E_2$ , is unphysical because the imaginary part of the energy is positive. But, as seen in this table, a rather small number of scattering states is enough to obtain reasonable values for the energies. Thus, at  $N_g = 35$  one already reaches a precision of the order of a few keV.

We have also performed similar calculations by using the single-particle states labelled WS2 in Table I, where the Fermi level is immersed in the continuum. Since the resonances are wider than before we used here a different one-particle contour, namely a=0.1 MeV, b=13 MeV, c=-6 MeV and d= 26 MeV.

The straight lines discussed above appear also in this case with the same characteristics as before. The remaining physical two-particle energies are shown in Fig. 4. The strengths  $G_\lambda$  in the figure are 10 % larger than the corresponding ones in the previous case.

The general features of the states in the continuum in this figure are similar to those in the previous one, as expected since these states are determined mainly by the Gamow resonances and the continuum background. In fact there is not any essential difference between the two calculations since within this formalism all states (including the continuum states) are treated on the same footing, independently of the location of the Fermi level. But due to the different single-particle states that enter in the calculation the bound states show an striking difference with the previous case. Thus, since there is not any bound single-

---

<sup>1</sup>Due to the Berggren metric the matrix representation of the Hamiltonian is not Hermitian in the complex energy sector.

particle state and the state  $2s_{1/2}$  is not present in this case, there is only one two-particle bound state which materializes only when the interaction is large enough. This occurs in the figure at  $G = 0.023$  MeV, where that bound state appears at an energy of -0.104 MeV. The main components of the corresponding wave function are  $(-0.95, 0.03)(1d_{5/2})^2 + (0.21, 0.00)(0h_{11/2})^2 + (-0.17, 0.07)(1d_{3/2})^2 + (-0.13, 0.01)(0g_{7/2})^2 + (0.11, -0.05)(1f_{7/2})^2$ . The interesting point is that this wave function does not change much as the interaction is increased, which shows the role played by the Gamow states in building up the bound states. The importance of these resonances is related to their widths. The wider the Gamow resonance the smaller is their influence. However, one cannot conclude from this that only Gamow resonances would be enough to describe the two-particle states of interest, since the inclusion of the complex contour is important to obtain even the narrow resonances and the bound states. In particular, without the contour the imaginary part of the energy corresponding to bound states becomes large, as it happened in the previous example.

In conclusion we have presented in this paper a method to perform shell model calculations in the continuum. We have shown that wide resonances and even the continuum background can be important to describe narrow two-particle resonances. We thus think that we have solved the old problem of describing microscopically resonances induced by a two-body interaction in the background of a many-body mean field.

#### ACKNOWLEDGMENTS

This work has been supported by FOMEC (Argentina), by the Hungarian OTKA fund Nos. T26244 and T29003, by the Swedish Foundation for International Cooperation in Research and Higher Education (STINT) and by the Swedish Institute.



## REFERENCES

- [1] F. M. Marqués et. al., Phys. Rev. C **64**, 61301(R) (2001), and references therein.
- [2] R. J. Liotta, E. Maglione, N. Sandulescu and T. Vertse, Phys. Lett. **367B**, 1 (1996).
- [3] T. Berggren, Phys. Lett. **B73**, 389 (1978).
- [4] R. G. Thomas, Prog. Theor. Phys. **12**, 253 (1954); R. G. Lovas et. al., Phys. Report **294**, 265 (1998).
- [5] T. Berggren and P. Lind, Phys. Rev. **C47**, 768 (1993).
- [6] A. L. Fetter and J. D. Walecka, Quantum theory of many-particle systems, McGraw-Hill, New York, 1971.
- [7] A. M. Lane, Nuclear theory, Benjamin Reading, Mass, 1964.
- [8] A. Evans et. al., Nucl. Phys. **A93**, 261 (1967).
- [9] G. F. Bertsch and H. Esbensen, Ann. of Phys. **209**, 327 (1991).
- [10] T. Vertse, K. F. Pál and Z. Balogh, Comput. Phys. Commun. **27**, 309 (1982).
- [11] L. Gr. Ixaru, M. Rizea and T. Vertse, Comput. Phys. Commun. **85**, 217 (1995).
- [12] N. Sandulescu, N. Van Giai and R. J. Liotta, Phys. Rev. C **61**, 61301(R) (2000).

## FIGURES

FIG. 1. (a) Rectangular one-particle contour in the complex energy plane. The points in this contour define the scattering functions that form the representation to be used in the two-particle basis. (b) Continue set of states in the two-particle energy plane (dashed region). The white area corresponds to the allowed region. The values of  $a$ ,  $b$ ,  $c$  and  $d$  are as in the one-particle contour of the previous figure.

FIG. 2. Poles in the two-particle energy plane corresponding to states  $\lambda=0$  in  $^{80}\text{Ni}$ . The labels of the straight lines correspond to configurations in which one of the two particles is in a bound state or a Gamow resonance and the other is on a scattering state. Energies are in MeV.

FIG. 3. Physically meaningful resonances in the two-particle energy plane plotted as a function of the energy gap  $\Delta$  (in MeV). The labels in each group of states indicate the zeroth-order configuration (i. e. at  $\Delta = 0$  MeV) corresponding to the group. Energies are in MeV.

FIG. 4. Poles in the two-particle energy plane corresponding to the case where the Fermi level lies in the continuum. The value of the strength  $G_\lambda$  (in MeV) was chosen as explained in the tex. The energies  $(E_r, E_i)$  defining the allowed region are constraint to the values  $0.2\text{MeV} < E_r < 13\text{MeV}$  and  $-6\text{MeV} < E_i < 0\text{MeV}$ . The labels in each group of levels indicate the zeroth-order configuration (i. e. at  $G = 0$ ) corresponding to the group. Energies are in MeV.

TABLES

TABLE I. Neutron single-particle states evaluated with the Woods-Saxon potential given in the text. The complex energies are in MeV. The column labelled *WS1* corresponds to  $V_0 = 40$  MeV while *WS2* to  $V_0 = 37$  MeV. The states  $0g_{9/2}$  are given to show the magnitude of the gap corresponding to the magic number  $N = 50$ .

state	WS1	WS2
$0g_{9/2}$	(-4.398,0)	(-2.587,0)
$1d_{5/2}$	(-0.800,0)	(0.294,-0.018)
$2s_{1/2}$	(-0.284,0)	-----
$1d_{3/2}$	(1.325,-0.479)	(1.905,-1.241)
$0h_{11/2}$	(3.296,-0.013)	(4.681,-0.069)
$1f_{7/2}$	(3.937,-1.796)	(4.455,-2.851)
$0g_{7/2}$	(4.200,-0.167)	(5.799,-0.506)

TABLE II. Energies (in MeV) of the  $\lambda = 0$  first excited bound state and of the lowest two-particle resonances in  $^{80}\text{Ni}$ . The discrete single-particle states are those labelled WS1 in Table I. The strength  $G_\lambda$  was chosen such that the energy gap is 1.4 MeV. The energies are given as a function of the number of scattering states included in the single-particle representation, i. e. the number  $N_g$  of Gaussian points. For  $N_g=0$  the representation consists of bound states and Gamow resonances only. The case  $N_g=225$  corresponds to the one used throughout the calculations presented here.

$N_g$	$E_1$	$E_2$	$E_3$	$E_4$
0	(-0.642,0.012)	(2.158,0.719)	(3.268,-0.883)	(7.931,-0.198)
35	(-0.65417,0)	(1.96874,-0.39235)	(3.92420,-1.05208)	(7.95693,-0.25236)
70	(-0.65274,0)	(1.96988,-0.39321)	(3.92429,-1.05159)	(7.95691,-0.25251)
110	(-0.65274,0)	(1.97261,-0.39838)	(3.92416,-1.05168)	(7.95687,-0.25250)
225	(-0.65308,0)	(1.97241,-0.39935)	(3.92390,-1.05189)	(7.95685,-0.25249)
550	(-0.65308,0)	(1.97241,-0.39935)	(3.92390,-1.05189)	(7.95685,-0.25249)

TABLE III. Wave function amplitude  $X((0h_{11/2})^2; E)$  corresponding to the resonances as labelled in Fig. 3. The energies  $E$  can be read from that figure. The values of the gap  $\Delta$  are given in MeV.

State	$\Delta = 0$	$\Delta = 0.6$	$\Delta = 1.2$	$\Delta = 1.4$	$\Delta = 1.7$
$d_{3/2}^2$	(0,0)	(0.20,-0.15)	(0.44,-0.08)	(0.48,-0.04)	(0.49,-0.00)
$h_{11/2}^2$	(1,0)	(0.92,0.02)	(0.78,0.05)	(0.75,0.03)	(0.71,0.00)
$g_{7/2}^2$	(0,0)	(-0.35,-0.02)	(-0.41,-0.02)	(-0.42,-0.02)	(-0.43,-0.02)
$f_{7/2}^2$	(0,0)	(-0.16,0.00)	(-0.20,0.02)	(-0.20,0.03)	(-0.21,0.03)

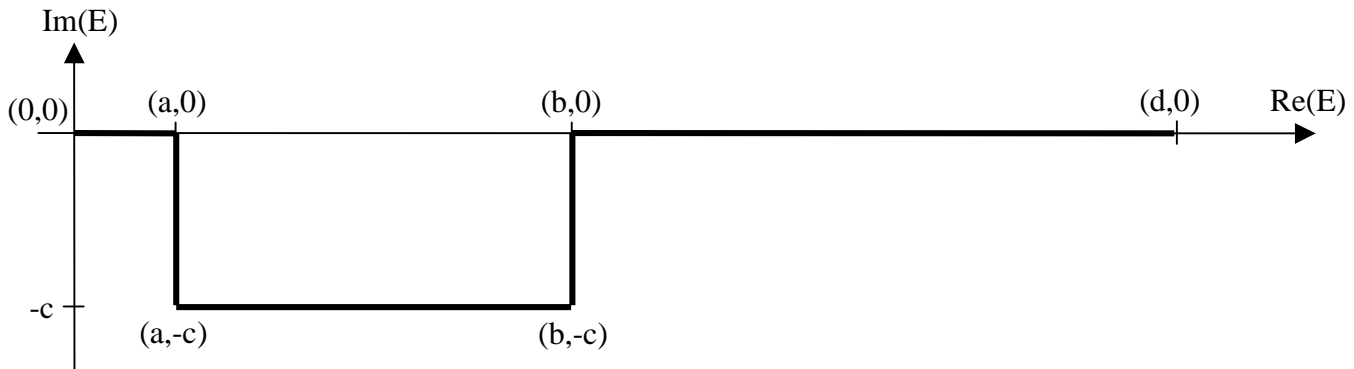


Fig. 1a

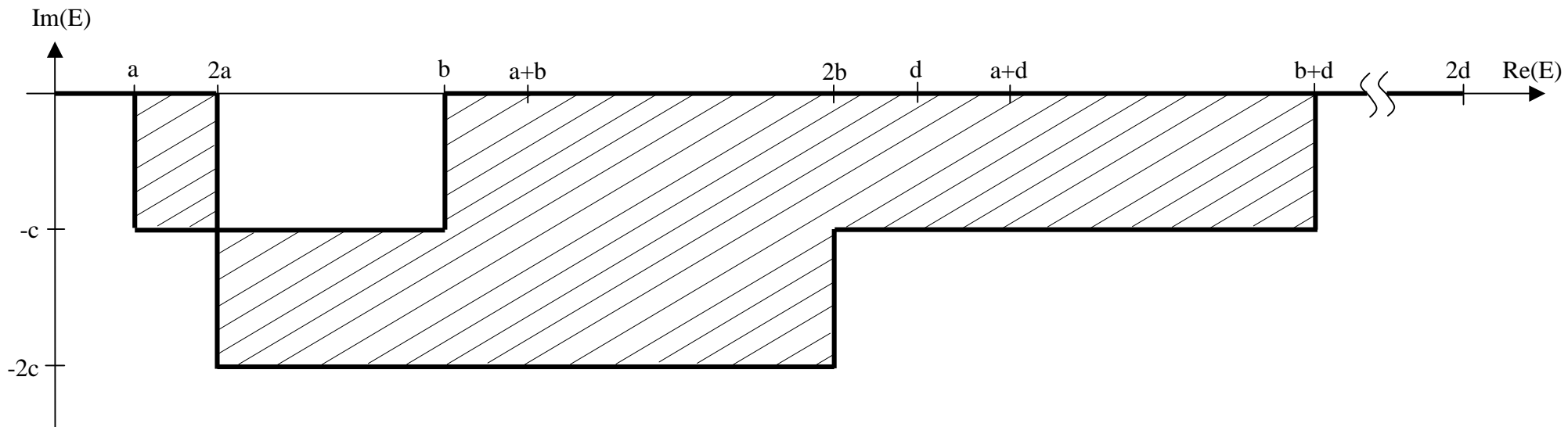


Fig. 1b

